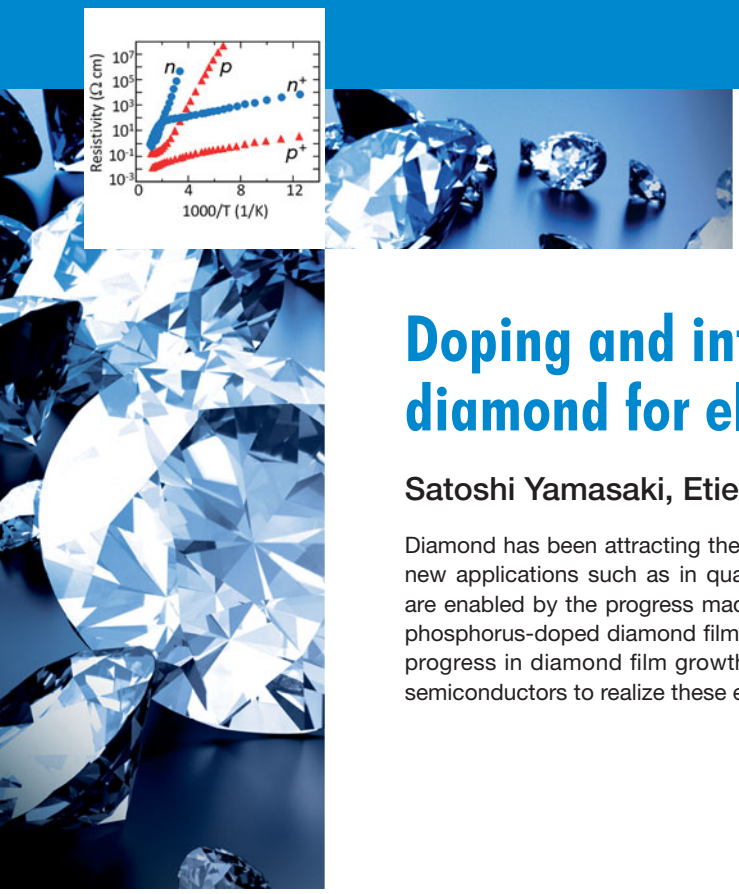

Doping and interface of homoepitaxial diamond for electronic applications

Satoshi Yamasaki, Etienne Gheeraert, and Yasuo Koide

Diamond has been attracting the attention of many researchers because of its potential for new applications such as in quantum devices and power electronics. These applications are enabled by the progress made in improving the quality of undoped, boron-doped, and phosphorus-doped diamond films grown by chemical vapor deposition techniques. Recent progress in diamond film growth and heterostructures of diamond and other compound semiconductors to realize these electronics applications are reported.

Introduction

Diamond is widely known as a superior material for electronics applications because of its high hardness, high thermal conductivity, and high breakdown voltage. Diamond Schottky junction diodes and field-effect transistors (FETs) are mainly being developed. In addition, diamond has unique properties for electronics applications such as extremely long spin relaxation times of point defects, negative electron affinity (NEA) of hydrogen terminated surfaces, stable exciton states at room temperature, and high conductivity for heavy doping. Using these unique properties, new types of electronic devices can be fabricated: room-temperature operating quantum devices by long spin-lattice relaxation times,[1,2] electron emission *p*-*i*-*n* (or *p*–*n*) diodes by NEA,[3,4] exciton light-emitting diodes by stable excitons,[5,6] and high current density diodes by hopping conduction in heavily doping diamond.[7,8] These achievements are made possible by success in high-quality diamond growth. In this article, we introduce recent progress in diamond film growth to realize electronics applications, including intrinsic and *n*-type doping of diamond, *p*-type doping of diamond, and heterostructures of diamond and other compound semiconductors.

Intrinsic and *n*-type doped diamond film growth

Research on diamond within the field of electronics has accelerated since the end of the 1990s when high-quality intrinsic and boron-doped *p*-type diamond was fabricated. High-quality diamond is homoepitaxially grown by the plasma-enhanced chemical vapor deposition (PECVD) technique on high temperature and high pressure diamond substrates. The typical growth conditions are a substrate temperature around 1000°C, pressure of 20–100 Torr, and microwave power of 200–5000 W. The source gas is hydrogen-diluted methane, and the dilution ratio is less than 1 vol%.[9–16]

For *p*-type diamond, boron as an impurity is easily incorporated into both natural and synthetic diamond by CVD without any restriction on crystal orientation. On the other hand, *n*-type diamond is not present in nature, and controlled *n*-type doping had been considered almost impossible until 1997.[17] Among the group V elements as dopants, nitrogen was one of the candidates for *n*-type doping because of its similar covalent bond length (0.074 nm) to that of diamond (0.077 nm), but it forms a deep donor level ~1.7 eV below the bottom of the conduction band due to its structural distortion from the substitutional position in the diamond lattice.

An important breakthrough was the success of P-doped *n*-type diamond by Koizumi et al.[17] They experimentally demonstrated the growth of P-doped *n*-type diamond on (111)-oriented diamond substrates by PECVD using a mixture of PH_3/CH_4 (concentration: 1,000–20,000 ppm) as a dopant source and H_2 gas. They carefully controlled the growth conditions to improve crystallinity and avoid undesirable impurities

Satoshi Yamasaki, National Institute of Advanced Industrial Science and Technology, Japan; s-yamasaki@aist.go.jp
Etienne Gheeraert, University of Grenoble Alpes, Institut NEEL, France; Etienne.gheeraert@neel.cnrs.fr
Yasuo Koide, National Institute for Materials Science, Japan; koide.yasuo@nims.go.jp
DOI: 10.1557/mrs.2014.100

such as hydrogen, boron, and nitrogen at specific P-doping concentrations. Following this success, much effort was devoted to growing high-quality P-doped, *n*-type diamond films,[12–15] so that nowadays, room-temperature mobility up to ~660 cm^2/Vs for a film with a phosphorus concentration of 7×10^{16} cm^{-3} has been achieved.[18] The phosphorus donor level in diamond was experimentally estimated at ~0.6 eV below the bottom of the conduction band.

The discovery of phosphorus doping of diamond was limited to the (111)-oriented diamond lattice structure. For actual technological applications, the growth of *n*-type diamond films on (001) substrates was a basic requirement because of an advantage regarding substrate size. In 2005, Kato et al. overcame this difficulty by optimizing the conditions for CVD growth, where the parameters differ significantly compared to those for (111) growth.[19,20] This is a significant achievement, eliminating the restrictions on crystal orientation of *n*-type doping. Based on this breakthrough, the fabrication of *p*–*n* or *p*-*i*-*n* junctions with good diode characteristics became feasible on (001)-oriented substrates with all CVD layers, and high-efficiency excitonic emission with deep UV light at room temperature could be realized.[6]

The deep dopant level of 0.6 eV for P-doping causes a serious issue for diamond electronic devices because of the small density of free carriers at room temperature (i.e., because of the high resistivity of the material). In order to decrease the resistivity, a heavy P-doping technique has been proposed.[7,8] Since the energy levels of dopants are very deep, even in a relatively high doping regime, these levels are separated from the extended states without overlap. Also, diamond has a strong C–C bonding energy, which reduces the defect creation probability one would expect from heavy doping. This is unique to diamond, because for other compound semiconductors, the resistivity increases with an increase in doping density in the doping proximity of 10^{19} cm^{-3}. For diamond, the resistivity monotonously decreases with increasing dopant density even over 10^{20} cm^{-3}. The conduction mechanism changes from band conduction to hopping conduction around 10^{19} cm^{-3}.[8]

At room temperature, in both *p*-type and *n*-type single crystal diamond, the resistivity can be largely reduced when hopping conduction dominates a conduction system.[8,9] **Figure 1** shows the temperature dependence of resistivity of B- and P-doped diamond films (*p*-type, *p*+-type, *n*-type, and *n*+-type; + means heavy doping). The doping concentrations of these films are 1×10^{18} cm^{-3}, 1×10^{20} cm^{-3}, 1×10^{18} cm^{-3}, and 8×10^{19} cm^{-3}, respectively. For *p*-type and *n*-type films over the entire temperature range and *n*+-type films (8×10^{19} cm^{-3}) in the high-temperature range (>500 K), thermally activated conduction (band conduction) has been observed originating from donor and acceptor levels of 0.6 eV and 0.37 eV from the conduction band minimum and the valence band maximum, respectively. On the other hand, the *n*+-type film in a low-temperature range and the *p*+-type film (1×10^{20} cm^{-3}) over the entire temperature range have a weaker temperature dependence, which originates from hopping conduction. As shown in Figure 1, *n*+- and *p*+-type films have much smaller resistivity than *n*- and *p*-type films at room temperature, respectively.

The film quality of diamond still continues to be improved and valency control in diamond is almost possible. It is a good time to develop high-performance diamond electronic devices.

p-type doping of diamond

Collins et al.[21] made the first clear demonstration of *p*-type behavior in some rare electricity-conducting diamond crystals in 1971. Aluminum was supposed to be the main acceptor in *p*-type diamond,[22] but it has been shown that boron is in fact the only *p*-type dopant that can be incorporated with high reproducibility into the diamond structure. Its activation energy of 382 meV is rather large compared to usual semiconductors, but substitutional boron behaves as a shallow level center, with the high value being consistent with the low dielectric constant and the large hole effective masses.[23] The covalent radii of boron (0.082 nm) and carbon (0.077 nm) are close enough to allow incorporation of boron into substitutional sites with high solubility.

The first attempts at boron doping from the gas phase were performed using diborane (B_2H_6), which, upon decomposition, allows an intake of boron atoms in the gas mixture and thus a possible reintroduction of these in the solid phase.[24] Subsequently, other attempts at *p*-doping diamond from the gas phase have been initiated from various other gaseous precursors such as trimethylborate ($B(OCH_3)_3$),[25] trimethylboron (TMB, $B(CH_3)_3$ that has a higher thermal stability compared to diborane),[26] and triethylbore ($B(C_2H_5)_3$).[27] Boron powder[28] and boron trioxide (B_2O_3) dissolved in ethanol[29] were also used as impurity sources. Currently, *p*-doping from the gas phase is done mainly using diborane and TMB. With diborane, a doping range of a few 10^{14} cm^{-3} [30] up to 10^{22} cm^{-3} [31] is possible in both monocrystalline and polycrystalline layers.[32]

Doping by ion implantation has poor efficiency, since defect recovery is very difficult both because of the high diffusion energies in diamond (requiring high annealing temperatures) and the metastable nature of diamond inducing a transformation into graphite after amorphization due to the implantation.[33]

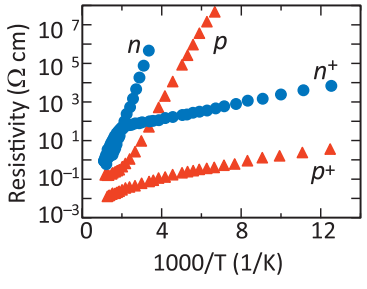

Figure 1. Temperature dependence of resistivity of B- and P-doped diamond films (*p*-type, *p*+-type, *n*-type, and *n*+-type).[8]

For boron concentrations lower than 2×10^{17} cm^{-3}, the hole concentration activation energy is around 370 meV. At higher boron concentrations, the activation energy decreases near the formation of a boron impurity band, which supplies additional near-neighbor hopping conduction at low temperature. At a boron concentration of 4.5×10^{20} cm^{-3}, metallic conduction is observed.[34] At room temperature, the phonon scattering mechanism governs the carrier mobility,[35] leading to an intrinsic mobility of 2000 cm^{2}V^{-1}s^{-1}, as reported by several groups for high-quality lightly doped diamond films,[9,36,37] see **Figure 2**. In the case of doping levels larger than 10^{17} cm^{-3}, the scattering induced by the ionized impurities becomes the dominant mechanism and reduces the mobility.[35]

The large ionization energy of boron results in low carrier concentration at room temperature and consequently high resistivity. This induces a series resistance in electronic devices, and careful design reducing this resistance as much as possible is required, such as a buried heavily doped layer with metallic conductivity. This also leads to low conductance of junction FETs. In order to enhance the carrier concentration, various solutions have been explored, such as a H-terminated transistor that creates hole accumulation on the surface easily controlled by a top gate,[38] or a delta-doped transistor benefitting from quantum confinement to enhance the hole mobility of a very thin metallic layer,[39] and, more recently, a metal oxide semiconductor (MOS) transistor working in the inversion regime.[40]

Heterointerface

For diamond, since activation energy of dopants is larger than 0.3 eV, conductivity control is required for the operation of diamond FETs. Two major approaches have been adopted for this. The first is a diamond FET obtained using a surface conductive layer on the hydrogen-terminated diamond surface.[41] The surface is easily prepared with hydrogen plasma treatment using a microwave plasma chemical vapor deposition (MPCVD) technique and is known to provide a two-dimensional hole gas (2DHG). The 2DHG achieves a hole channel with a typical sheet carrier density of 10^{13} cm^{-2} and Hall mobility ranging from 50 to 150 cm^2/V•s. These FETs have been widely studied, and the term surface-channel FETs has been coined. Although several models have been proposed to explain the formation of the 2DHG, an exact understanding of the mechanism is still being investigated. Although surface-channel FETs have a high possibility for application in high-frequency and high-power FETs, their properties are significantly affected by their surrounding environment due to the lack of a protective layer that does not degrade the 2DHG. Thus, it has been necessary to explore passivation layers to stabilize device performance.

The second approach toward conductivity control is a diamond FET using a heavily boron-doped layer prepared with delta-doping (with thickness below 1 nm and a doping level larger than 10^{20} cm^{-3}) based on the MPCVD technique.[42] It is predicted that a delta-doped layer is required to control the FET action. Therefore, FET performance is still in the preliminary stage, and further development of the delta-doping technique is a key factor for successful fabrication of diamond FETs.

Thus, it is important to search for a new approach that provides thermally stable, high-frequency, and high-power diamond FETs. A combination of diamond and other semiconductors or dielectrics using a "heterointerface" is a possible strategy for producing such electronic devices. Miskys et al.[43] made the first demonstration of the AlN/diamond heterojunction diode by using a molecular beam epitaxy (MBE) technique, and an epitaxial AlN layer was obtained on the diamond substrate surface. Kueck et al.[44] reported on the effectiveness of AlN for passivating a hydrogen-terminated diamond surface. Group-III nitrides (AlN, GaN, and BN) with wide energy bandgaps are attractive materials for diamonds. Since it is difficult to grow GaN directly on diamond surfaces, AlN and BN are key materials for fabricating heterojunction FETs (HFETs). Imura et al.[45] demonstrated the first AlN/diamond HFET prepared by a metal organic vapor phase epitaxy technique.

The other approach to prepare a heterointerface is in dielectrics. In order to achieve high-current output FETs, strong coupling between the gate capacitance and the conductive channel is required. Simultaneously, a valence band offset, ΔE_V, between the diamond and dielectric is important to accumulate holes in diamond

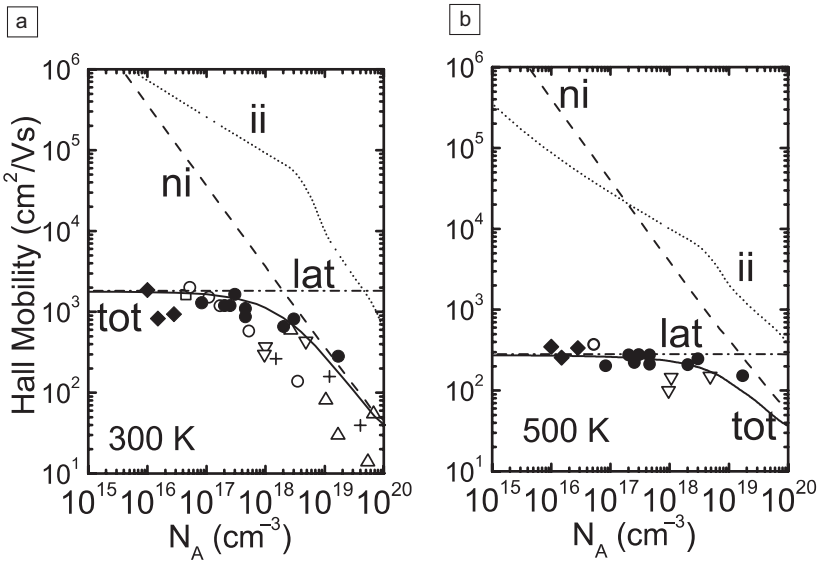

Figure 2. Hall mobility of holes as a function of doping level in homoepitaxial diamond at (a) 300 K and (b) 500 K. The symbols indicate experimental data, and the theoretical contributions of various scattering modes are illustrated by dashed and dotted lines for the lattice (lat, acoustic, and optical phonons): a dotted line for the ionized impurities (ii) mode, and a dashed line for the neutral impurities (ni) mode.[35]

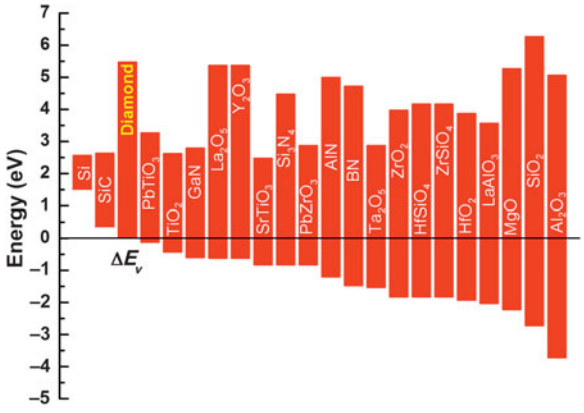

Figure 3. Energy band lineup for various semiconductors, Group III nitrides, and oxides, where the zero energy equals the diamond valence band edge. The graph is compiled using the values simulated by Mönch and Robertson.[46,47]

close to the interface. **Figure 3** shows a band lineup evaluated by the charge neutrality level for various semiconductors, III-nitrides, and oxides, where the zero energy equals the diamond valence band edge.[46,47] A ΔE_V value larger than 1 eV is needed to obtain the hole accumulation stage. Various gate dielectrics such as SiO_2,[48] Al_2O_3,[49] CaF_2,[50] Ta_2O_5,[51] HfO_2,[52] and $LaAlO_3$[53] were developed for the fabrication of MOS diodes and MOSFETs.

Figure 4 shows real charge and hole densities in diamond as a function of the electric field, which is applied to the gate dielectric. The charge density can be controlled by SiO_2, Al_2O_3, and CaF_2 and is lower than 1 μC/cm^2, which corresponds to a hole density around 1×10^{13} cm^{-2} at an applied electric field lower than 2 MV/cm, since the dielectric constants (k) of these dielectrics are lower than 10. A gate dielectric with $k > 100$ is essential to control the hole density around 1×10^{14} cm^{-2} reported for a hydrogen-terminated surface (see the blue dot point in Figure 4),[51] and therefore ferroelectric materials represent a good choice of gate dielectric. The reduction in thickness of the gate

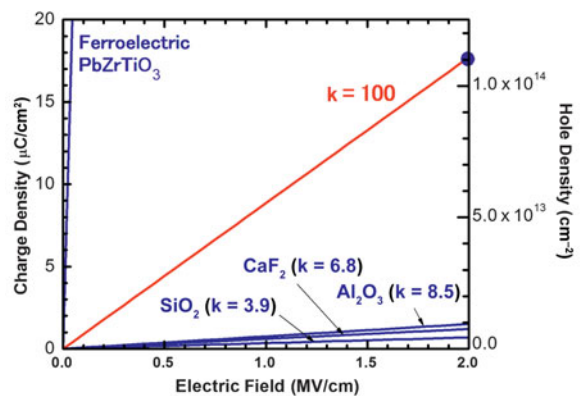

Figure 4. Charge and hole densities in diamond as a function of electric field that is applied to gate dielectrics.[51]

dielectric to obtain a large charge density provides an increase in the leakage current that originates from carriers tunneling through the gate dielectrics. A gate insulator with higher dielectric constant (high-k) is desirable for the development of diamond FET.

Conclusion

Excellent heterointerfaces and heterojunctions are key to the successful development of high-performance diamond electron devices, and III-nitrides and high-k oxides are good candidate materials to realize these devices. Our research direction has been to search for the best gate material for diamond HFET and MOSFET.

Because diamond has superior and unique properties, we expect new types of electronic devices to emerge, which cannot be achieved using other semiconductors. To realize such electronic devices, further progress in substrate size, crystallinity, doping technique, interface control, and surface control will be important.

References

1. A. Gruber, A. Dräbenstedt, C. Tietz, L. Fleury, J. Wrachtrup, C. von Borczyskowski, *Science* **276**, 2012 (1997).
2. N. Mizuochi, T. Makino, H. Kato, D. Takeuchi, M. Ogura, H. Okushi, M. Nothaft, P. Neumann, A. Gali, F. Jelezko, J. Wrachtrup, S. Yamasaki, *Nat. Photonics* **6**, 299 (2012).
3. S. Koizumi, T. Ono, T. Sakai, *Japan New Diamond Forum* 262 (2006).
4. D. Takeuchi, T. Makino, H. Kato, H. Okushi, S. Yamasaki, *Phys. Status Solidi A* **208**, 2073 (2011).
5. S. Koizumi, K. Watanabe, M. Hasegawa, H. Kanda, *Science* **292**, 1899 (2001).
6. T. Makino, H. Kato, M. Ogura, H. Watanabe, S.G. Ri, S. Yamasaki, H. Okushi, *Jpn. J. Appl. Phys.* **44**, L1190 (2005).
7. H. Kato, H. Umezawa, N. Tokuda, D. Takeuchi, H. Okushi, S. Yamasaki, *Appl. Phys. Lett.* **93**, 202103 (2008).
8. K. Oyama, S.-G. Ri, H. Kato, M. Ogura, T. Makino, D. Takeuchi, N. Tokuda, H. Okushi, S. Yamasaki, *Appl. Phys. Lett.* **94**, 152109 (2009).
9. S. Yamanaka, H. Watanabe, S. Masai, D. Takeuchi, H. Okushi, K. Kjimura, *Jpn. J. Appl. Phys.* **37**, L1129 (1998).
10. Y.G. Chen, M. Ogura, H. Okushi, *Appl. Phys. Lett.* **82**, 4367 (2003).
11. T. Teraji, *Phys. Status Solidi A* **203**, 3324 (2006).
12. H. Kato, W. Futako, S. Yamasaki, H. Okushi, *Diam. Relat. Mater.* **13**, 2117 (2004).
13. M. Nesladek, *Semicond. Sci. Technol.* **20**, R19 (2005).
14. A. Tajani, E. Gheeraert, N. Casanova, E. Bustarret, J.A. Garrido, G. Rumen, C.E. Nebel, M.E. Newton, D. Evans, *Phys. Status Solidi A* **193**, 541 (2002).
15. T. Kociniewski, J. Barjon, M.A. Pinault, F. Jomard, A. Lusson, D. Ballutaud, O. Gorochov, J.M. Laroche, E. Rzepka, J. Chevallier, C. Saguy, *Phys. Status Solidi A* **203**, 3136 (2006).
16. J. Isberg, J. Hammersberg, E. Johansson, T. Wikström, D.J. Twitchen, A.J. Whitehead, S.E. Coe, G.A. Scarsbook, *Science* **297**, 1670 (2002).
17. S. Koizumi, M. Kamo, Y. Sato, H. Ozaki, T. Inuzuka, *Appl. Phys. Lett.* **71**, 1065 (1997).
18. M. Katagiri, J. Isoya, S. Koizumi, H. Kanda, *Appl. Phys. Lett.* **85**, 6365 (2004).
19. H. Kato, S. Yamasaki, H. Okushi, *Appl. Phys. Lett.* **86**, 222111 (2005).
20. H. Kato, T. Makino, S. Yamasaki, H. Okushi, *J. Phys. D: Appl. Phys.* **40**, 6189 (2007).
21. A.T. Collins, W.S. Williams, *J. Phys. C: Solid State Phys.* **4**, 1789 (1971).
22. R.M. Chrenko, *Phys. Rev. B: Condens. Matter* **7**, 4560 (1973).
23. E. Gheeraert, S. Koizumi, T. Teraji, H. Kanda, M. Nesladek, *Phys. Status Solidi A* **174**, 39 (1999).
24. N. Fujimori, T. Imai, A. Doi, *Vacuum* **36**, 99 (1986).
25. C.F. Chen, S.H. Chen, T.M. Hong, T.C. Wang, *Diam. Relat. Mater.* **3**, 632 (1994).
26. J. Cifre, J. Puigdollers, M.C. Polo, J. Esteve, *Diam. Relat. Mater.* **3**, 658 (1994).
27. R. Haubner, S. Bohr, B. Lux, *Diam. Relat. Mater.* **8**, 171 (1999).
28. T.H. Borst, O. Weis, *Diam. Relat. Mater.* **4**, 948 (1995).
29. Y. Show, T. Matsukawa, H. Ito, M. Iwase, T. Izumi, *Diam. Relat. Mater.* **9**, 337 (2000).
30. P.-N. Volpe, P. Muret, J. Pernot, F. Omnès, T. Teraji, Y. Koide, F. Jomard, D. Planson, P. Brosselard, N. Dheilly, B. Vergne, S. Scharnholz, *Appl. Phys. Lett.* **97**, 223501 (2010).

31. E. Bustarret, P. Achatz, B. Sacepe, C. Chapelier, C. Marcenat, L. Ortega, T. Klein, *Philos. Trans. R. Soc. London, Ser. A* **366**, 267 (2008).
32. Y. Takano, M. Nagao, T. Takenouchi, H. Umezawa, I. Sakaguchi, M. Tachiki, H. Kawarada, *Diam. Relat. Mater.* **14**, 1936 (2005).
33. F. Fontaine, C. Uzan-Saguy, B. Philosoph, R. Kalish, *Appl. Phys. Lett.* **68**, 2264 (1996).
34. T. Klein, P. Achatz, J. Kacmarcik, C. Marcenat, F. Gustafsson, J. Marcus, E. Bustarret, J. Pernot, F. Omnes, B.E. Sernelius, C. Persson, A. Ferreira da Silva, C. Cytermann, *Phys. Rev. B: Condens. Matter* **75**, 165313 (2007).
35. J. Pernot, P.N. Volpe, F. Omnes, P. Muret, V. Mortet, K. Haenen, T. Teraji, *Phys. Rev. B: Condens. Matter* **81**, 205203 (2010).
36. T. Teraji, H. Wada, M. Yamamoto, K. Arima, T. Ito, *Diam. Relat. Mater.* **15**, 602 (2006).
37. V. Mortet, M. Daenen, T. Teraji, A. Lazea, V. Vorlicek, J. D'Haen, K. Haenen, M. D'Olieslaeger, *Diam. Relat. Mater.* **17**, 1330 (2008).
38. H. Kawarada, *Jpn. J. Appl. Phys.* **51**, 090111 (2012).
39. G. Chicot, T.N. Tran Thi, A. Fiori, F. Jomard, E. Gheeraert, E. Bustarret, J. Pernot, *Appl. Phys. Lett.* **102**, 162101 (2012).
40. G. Chicot, A. Marechal, R. Motte, P. Muret, E. Gheeraert, J. Pernot, *Appl. Phys. Lett.* **102**, 242108 (2013).
41. H. Kawarada, M. Aoki, M. Ito, *Appl. Phys. Lett.* **65**, 1563 (1994).
42. A. Aleksov, A. Vescan, M. Kunze, P. Gluche, W. Ebert, E. Kohn, A. Bergmaier, G. Dollinger, *Diam. Relat. Mater.* **8**, 941 (1999).
43. C. Miskys, J. Garrido, C. Nebel, M. Hermann, O. Ambacher, M. Stutzmann, *Appl. Phys. Lett.* **82**, 290 (2003).
44. D. Kueck, J. Scharpf, W. Ebert, M. Fikry, F. Scholz, E. Kohn, *Phys. Status Solidi A* **207**, 2035 (2010).
45. M. Imura, R. Hayakawa, E. Watanabe, M.Y. Liao, Y. Koide, H. Amano, *Phys. Status Solidi RRL* **5**, 125 (2011).
46. W. Mönch, *J. Appl. Phys.* **80**, 5076 (1996).
47. J. Robertson, *J. Vac. Sci. Technol.* **18**, 1785 (2000).
48. T. Saito, K.H. Park, K. Hirama, H. Umezawa, M. Satoh, H. Kawarada, Z.Q. Liu, K. Mitsuishi, K. Furuya, H. Okushi, *J. Electron. Mater.* **40**, 247 (2011).
49. K. Hirama, H. Sato, Y. Harada, H. Yamamoto, M. Kasu, *Jpn. J. Appl. Phys.* **51**, 090112 (2012).
50. Y. Otsuka, S. Suzuki, S. Shikama, T. Maki, T. Kobayashi, *Jpn. J. Appl. Phys.* **34**, L551 (1995).
51. S.H. Cheng, L.W. Sang, M.Y. Liao, J.W. Liu, M. Imura, H.D. Li, Y. Koide, *Appl. Phys. Lett.* **101**, 232907 (2012).
52. J.W. Liu, M.Y. Liao, M. Imura, Y. Koide, *Appl. Phys. Lett.* **103**, 092905 (2013).
53. J.W. Liu, M.Y. Liao, M. Imura, H. Oosato, E. Watanabe, A. Tanaka, H. Iwai, Y. Koide, *J. Appl. Phys.* **114**, 084108 (2013). □